

# Novel Approach to Constructing an Ultra Low Cost Flowcell Biosensor

THESIS

Presented to the Faculty of the Department of Physics and Astronomy  
in Partial Fulfillment of the Major Requirements  
for the Degree of

BACHELOR OF SCIENCE IN  
PHYSICS

Jeffery Summers

May 2019

©2019 Middle Tennessee State University

All rights reserved.

The author hereby grants to MTSU permission to reproduce  
and to distribute publicly paper and electronic  
copies of this thesis document in whole or in part  
in any medium now known or hereafter created.

Novel Approach to Constructing an Ultra Low Cost Flowcell Biosensor

Jeffery Summers

Signature of Author:

---

Department of Physics & Astronomy

May 2019

Certified by:

---

Dr. William Robertson

Department of Physics & Astronomy

Thesis Supervisor

Accepted by:

---

Dr. Ronald Henderson

Professor of Physics & Astronomy

Chair, Physics & Astronomy

# ABSTRACT

In this thesis we present our approach to constructing an ultra low-cost flowcell biosensor. Our sensor is capable of detecting changes in index of refraction on the order of  $10^{-5}$ , showing that it is well suited for not only index testing but also for surface loading type processes where binding between molecules may occur. Our sensor utilizes 3D printed parts, a one dimensional photonic crystal coupled to a glass prism (rather than a traditional SPR metal-film-prism coupling system), and a CCD to operate. Bloch Surface Waves (BSWs) can be excited in the outer layer of our multilayer by coupling an incident laser beam to the prism-multilayer structure and the position of the BSWs can be tracked by analyzing the reflected beam. By using this method we are able to bring the cost of manufacturing the sensor to about \$100, excluding the photonic crystals which can be fabricated commercially. The largest cost of our system is the CCD used to collect data.

# TABLE OF CONTENTS

	Abstract . . . . .	iii
I.	Introduction . . . . .	1
II.	Experimental Design . . . . .	4
III.	Methods . . . . .	5

## LIST OF FIGURES

1	Surface Plasmon Resonance setup . . . . .	1
2	The laser on the right side of the image couples into the prism-multilayer structure atop the centerpiece and is then reflected into a CCD where data can be taken. . . . .	2

# I. INTRODUCTION

Flowcell sensors have many applications; disease detection, refractive index measurements and measurements of reactivity to name a few. These sensors have been operating on the basis of electromagnetic surface phenomena for decades. Most flowcells on the market work by exploiting surface plasma oscillations (SPOs). These oscillations are highly sensitive to changes in the optical properties of the adjacent medium and follow from Maxwell's equations when the dielectric functions of each medium satisfy the relation [?]

$$\frac{\epsilon_{spo}}{\epsilon_{adjacent}} < -1$$

Metals like aluminum, copper, gold, and silver have negative dielectric functions at wavelengths in the red/infrared [], so films of these metals are used as to generate SPOs in most flowcell sensors via a process known as Surface Plasmon Resonance (SPR). An SPR system utilizes light-prism coupling to excite the surface electrons on a thin metal film deposited on the hypotenusal face of the prism. A dark band representing the photons absorbed by the

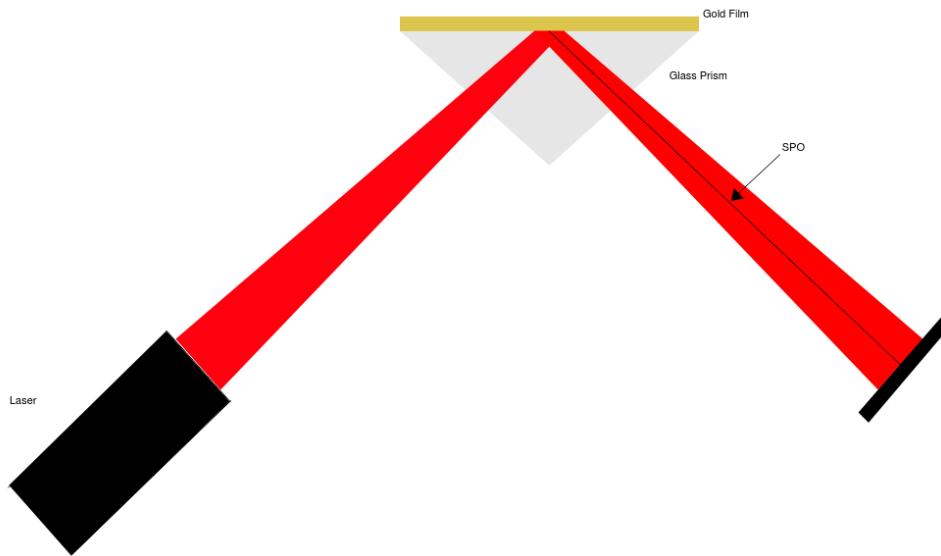


Figure 1: Surface Plasmon Resonance setup

surface electrons appears on the reflected beam image as seen in figure 1. There are quite a few drawbacks for using metal films, however. Metals are highly reactive so each time an SPR system is used a new prism must be used. These films also require particular wavelengths of incident light to excite the oscillations. Rather than using metal films, one-dimensional photonic crystals, or multilayers, can be designed to exhibit the phenomenon of surface electromagnetic waves (SEWs) or Bloch surface waves (BSWs), named after the physicist Felix Bloch who was famous for working with periodic systems. These surface waves have the same practical application as SPOs.

Multilayers overcome both of the shortcomings of metal films listed here. They can be designed to work for any wavelength and are typically made of nonreactive glass. In addition to these benefits, we expect that our 3-D printed and multilayer-based flowcell sensor will be more sensitive and precise with its measurements and be far cheaper to both build and maintain compared to traditional SPR sensors.

To take measurements with our sensor we look at the reflected image of incident laser light which has been coupled into the prism-multilayer interface to produce a BSW in the terminating layer. Our multilayer is designed to trap incident light in the last layer at a special angle; this results in a dark band in our reflected image. A diagram of the sensor is shown below.

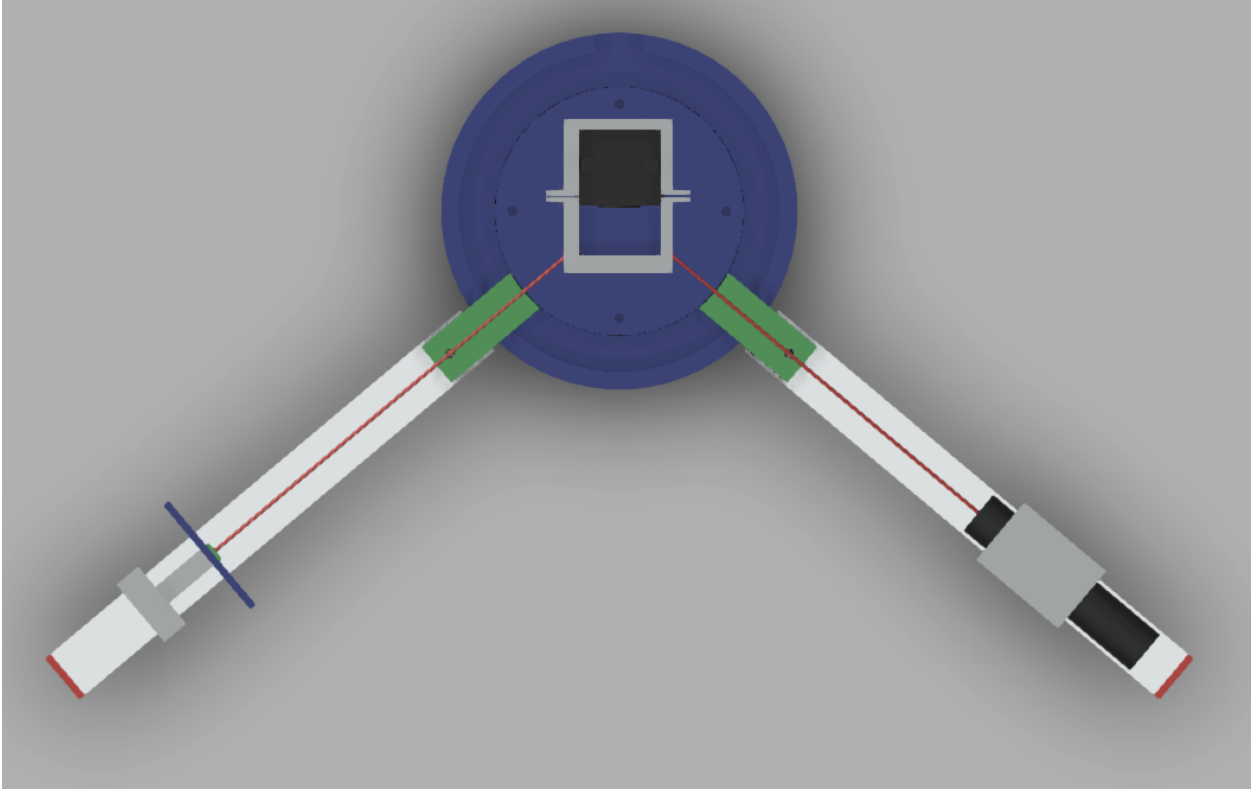


Figure 2: The laser on the right side of the image couples into the prism-multilayer structure atop the centerpiece and is then reflected into a CCD where data can be taken.

As fluids or gases are put into the flowcell chamber the index of refraction,  $n_c$ , changes. The condition for total internal reflection, found from Snell's law, for the interface between a glass prism and some transmitting medium whose index of refraction varies with time is given by:

$$\sin \theta_c = \frac{n_c(t)}{n_g}$$

We obtain an expression for the angle of reflection as a function of time by the Law of Reflection:

$$\theta_r(t) = \arcsin \frac{n_c(t)}{n_g}$$

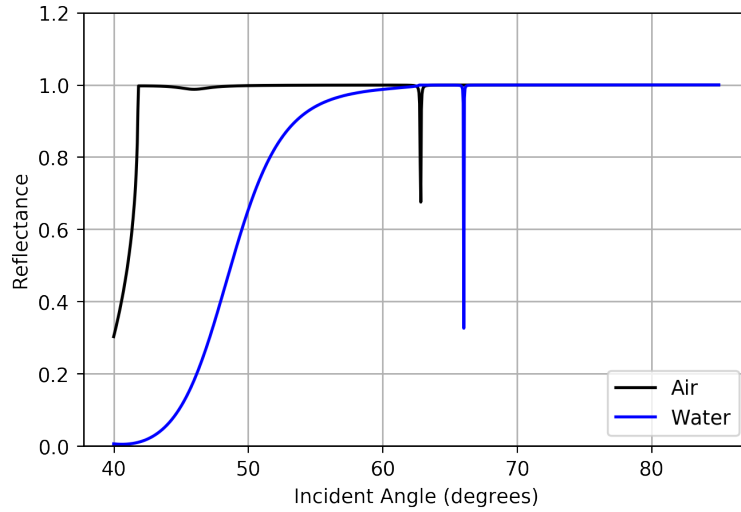
Note that this expression is valid for a single interface and hence does not accurately reflect our setup as we use a multilayer that behaves much differently than a single interface. With that said, this expression for  $\theta_r$  does capture the essence of our setup; the reflected angle (this is equivalent to the position of the surface mode) is a dependent on the index of refraction of the chamber. Using this fact we can associate variations in the flowcell chamber's index of refraction with differences in the BSWs angular position. These angular differences can be calculated by tracking the variation in the position of the dark band in the reflected image. A detailed analysis relating a shift in pixels on the CCD to the angular variation of the surface mode is listed in the methods section.



## **II. Experimental Design**

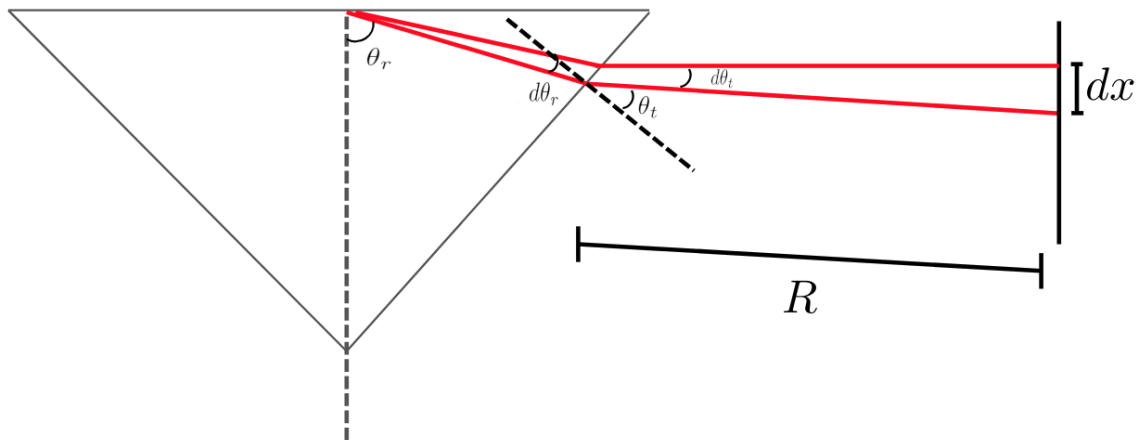
### III. Methods

To collect data from our biosensor we first prepare the flowcell chamber with the correct substrate or liquid that acts as our reference point for measuring changes in optical properties. After the chamber is prepared we then turn on the beam and rotate it until the special angle is reached.



As the index of refraction inside the flowcell chamber changes the dark band will translate left or right in our reflected image, depending on whether the index is increasing or decreasing. The shift in location of the band, in pixels, corresponds to an angular shift in the part of the reflected beam giving rise to the dark band. This is shown clearly in ?? as we see that a change from an index of 1.00 (air) to 1.33 (water) corresponds to an angular shift of about 3°.

Using the calculated data we can build a model to relate the index of refraction in the chamber to a shift in pixels on our CCD. To construct this relation we require Snell's law and some geometry. Using the classic formula for arclength and the diagram below we find:



$$dx = R d\theta_t$$

Using Snell's law we find

$$\theta_t = \arcsin(\sin(n_g \theta_r))$$

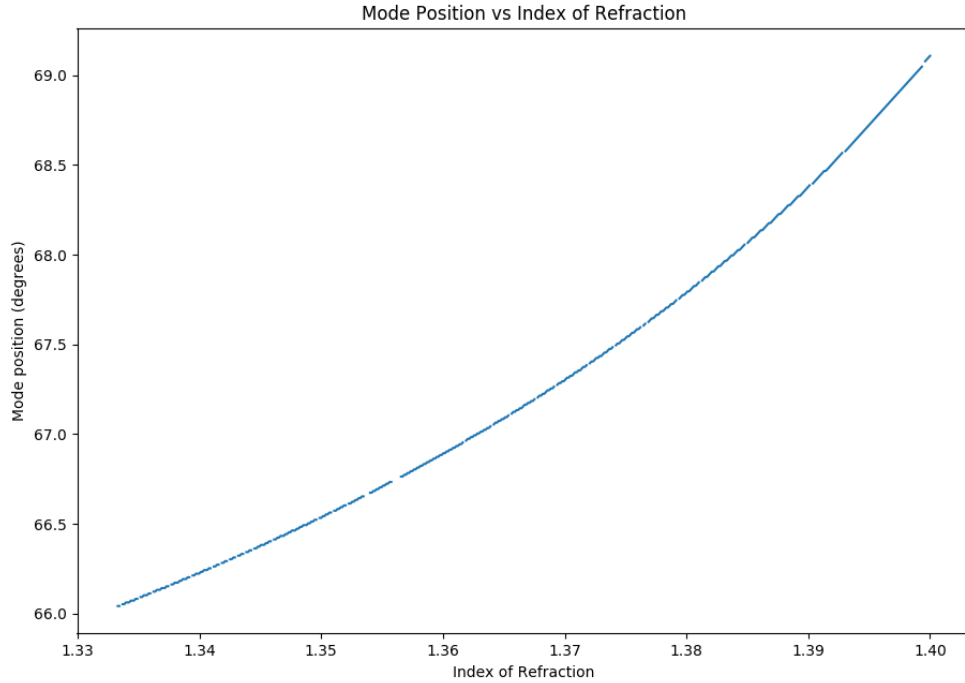
Which implies that

$$\begin{aligned} d\theta_t &= d(\arcsin(n_g \sin \theta_r)) \\ &= \frac{n_g \cos \theta_r}{\sqrt{1 - n_g^2 \sin^2(\theta_r)}} d\theta_r \end{aligned}$$

This leaves us with the relation between pixel shift and angular shift:

$$dx = \frac{R n_g \cos \theta_r}{\sqrt{1 - n_g^2 \sin^2(\theta_r)}} d\theta_r \quad (1)$$

Numerically we can determine the relationship between the reflected angle and the index inside the chamber. I wrote a python program to do just that for our multilayer, assuming the chamber is initially filled with water, and a graph of mode position ( $\theta_r$ ) vs index of refraction is plotted below.



## IV. RESULTS

The table below lists the mixtures of ethanol used to test for a change in index of refraction (\*This initial data is poorly measured and more data is being taken\*). The plot below shows the different indices of refraction corresponding to mixture A being injected over the interval [45.0, 55.0]. Similarly mixture B was injected over the interval [60.0, 75.0], and mixture C over [85.0, 95.0]. The dip in mode position is not expected over the first two intervals as we expect the mode to shift horizontally if the index of refraction in the chamber becomes larger than the original. However, the water used had been sitting in a syringe for a few days and may have actually increased in index of refraction, meaning that the index of the water in the chamber before injecting the first mixture may have been higher than the first two mixtures.

From this data we can infer a change in index of refraction of the medium once the index values of each mixture is known.

Mixtures	A	B	C
Ethanol (ml)	10.0	20.0	30.0
Water (ml)	100.0	100.0	100.0
Index	1.3380	1.3418	1.3450

